

Convective Merging of Vortex Cores in Lift-Generated Wakes

Vernon J. Rossow*

NASA Ames Research Center, Moffett Field, Calif.

The several wake vortices that originate from aircraft wingtips, flap edges, engine pylons, etc. usually merge, in the far field to form a single pair, whose structure determines the hazard posed to encountering aircraft. In order to gain an understanding of the process whereby vortices merge and disperse, a numerical study was made of the interaction of two-dimensional, time-dependent, inviscid vortical regions. It was found that discrete boundaries, which depend on the structure and spacing of the vortices, distinguish merging from nonmerging situations. Furthermore, certain arrays of finite vortex cores that alternate in sign were found to undergo division and merging that may be useful in alleviating the hazard posed by aircraft wakes.

Nonmenclature

AR	= aspect ratio
b	= wing span
C_L	= lift coefficient, lift / $[(1/2)\rho U_\infty^2 S]$
C_l	= local lift coefficient
C_l	= rolling-moment coefficient, rolling moment / $[(1/2)\rho U_\infty^2 Sb]$
c	= wing chord
\bar{c}	= mean geometric chord
d_e	= effective diameter of vortical region = $7 d_v / 6$
d_i	= spacing between centers of innermost vortices
d_s	= spacing between vortex centers
d_v	= diameter of outer ring of point vortices in vortical region = $2r_v$, with d_v arbitrarily set at $0.3 b$
k	= vortex core structure parameter
$\ell(y)$	= local spanwise lift
N	= number of vortices
r	= radius
S	= wing area
T	= dimensionless time = $4t\Gamma_v/b^2 = 0.36t\Gamma_v/d_v^2$
t	= time
U_∞	= freestream velocity; aligned with x axis
u, v, w	= velocity components in x, y , and z directions
v_θ	= circumferential velocity
V_{sh}	= wind-shear parameter [see Eq. (3)]
Wr	= Kirchhoff-Routh path function [see Eq. (5)]
X, Y, Z	= dimensionless coordinates, for example, $X = 2x/b = 0.6x/d_v$
x, y, z	= coordinates, x is streamwise and z is vertical
α	= angle of attack
Γ	= circulation
γ	= circulation in point vortices
ρ	= air density

Subscripts

f	= following model that encounters wake
g	= model that generates wake
v	= vortex or vortical region

Received June 28, 1976; presented as Paper 76-415 at the AIAA 9th Fluid and Plasma Dynamics Conference, San Diego, Calif., July 14-16, 1976; revision received Sept. 13, 1976.

Index categories: Aircraft Aerodynamics (including Component Aerodynamics); Jets, Wakes, and Viscid-Inviscid Flow Interactions; Aircraft Flight Operations.

*Staff Scientist, Associate Fellow, AIAA.

†The terms vortex, vortical region, and core are used interchangeably here to denote a region that contains vorticity.

Introduction

THE combination or merger of vortices shed by one side of a wing into a single vortex † is a common and well-known occurrence. It has only recently been shown, however, that the manner in which the vortices combine determines whether the wake will have its circulation concentrated (with high rotational velocities) or dispersed. It was first demonstrated in ground-based facilities¹⁻³ and then confirmed in flight⁴ that both kinds of wakes could be achieved with the Boeing 747 transport aircraft. The tests indicated that the rolling moment induced on an aircraft when it encounters the wake of the conventional landing configuration was about twice that of the modified landing configuration. This difference was attributed to the way in which the wake vortices merged behind the two configurations (Fig. 1). In the conventional wake, the vortices merge close behind the wing to form a single pair, has high rotational velocities and persists. The multiple vortices shed by the modified landing ($30^\circ/0^\circ$) configuration first combine across the inboard flap, and then this residue flap vortex and the wing-tip vortex merge to form a diffuse vortex that has low rotational velocities. The particular spacing between the vortices and the relative strengths required for such an interaction to occur were somewhat fortuitous occurrences on the B 747. If, therefore, this alleviation concept is to be extended to reduce wake velocities even further, and if it is to be applied to other aircraft, the design parameters for when and how vortices merge to form a dispersed wake must be determined.

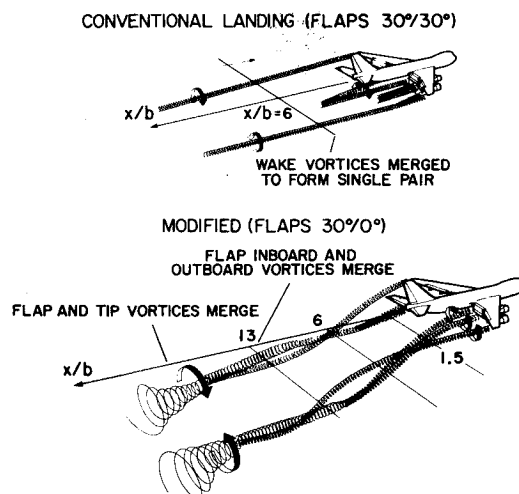


Fig. 1 Comparison of two wakes of Boeing 747.

The investigation reported here extends previous studies⁵⁻¹² of vortex merger and dispersion by considering a wider variety of vortex arrangements which relate to lift-generated wakes. The objective is first to develop guidelines for vortex interactions and then to find those arrangements that are particularly effective in causing the circulation in the wake to be dispersed or to combine in groups with nearly zero net circulation so that the wake is neutralized.

Development of Merging Guidelines

Initial Structure of Vortical Regions

The sections that follow each treat a particular arrangement of vortical regions or cores. Since the initial or starting conditions are somewhat arbitrary, it was decided to standardize the vortical regions so that each of them is initially axially symmetric and their centers are colinear. The distribution of vorticity in each core is simulated by placing point vortices at equal intervals on three concentric circles of radius $r_v/3$, $2r_v/3$, and r_v , where r_v is the radius of the outer ring of vortices in the vortical region. When all of the vortices are of the same strength, the approximately uniform spatial distribution approximates a Rankine vortex core. More concentrated vortices are simulated by making the point vortices on the inner rings stronger than those on the outer ones. The relationship used herein to obtain a systematic variation in core structure is developed as follows: The total circulation in the vortical region is given by

$$\Gamma_v = \gamma_1 n_1 + \gamma_2 n_2 + \gamma_3 n_3 \quad (1)$$

where, throughout this study, the number of vortices on each ring are set at $n_1=6$, $n_2=12$, and $n_3=18$, so that the distribution is approximately uniform. The strengths of the point vortices on circles 1, 2, and 3 are represented by γ_1 , γ_2 , and γ_3 . The circulation contained in each ring of vortices then is assumed to be represented by some power k of the radius of the circles.

$$\gamma_1 n_1 = C/(r_v/3)^k \quad \gamma_2 n_2 = C/(2r_v/3)^k \quad \gamma_3 n_3 = C/(r_v)^k$$

The strengths of the point vortices on the i th ring then are given by

$$\gamma_i = \Gamma_v / \{n_i (n_i/6)^k [1 + (1/2)^k + (1/3)^k]\} \quad (2)$$

When $k = -1$, the γ_i are all of the same strength, so that a Rankine vortex is simulated. As k increases, the vortices on the inner ring become stronger relative to those on the outer rings to simulate more concentrated vortices; this is indicated in Fig. 2 by the radial variations in circulation for $k = -1$ through $+4$. The large dots on the curves indicate the locations of the vortex rings. In all cases considered, the circulation in the strongest vortex was given by $\Gamma_v = 3.6 b U_\infty$ to insure control of numerical error.

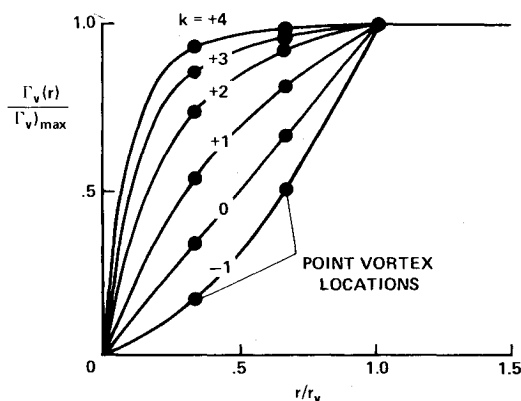


Fig. 2 Radial variation of circulation in vortex cores to be studied as simulated by point vortex representation.

Once the initial configuration of vortices was set up, their subsequent motions were calculated by using the numerical technique and the error monitoring parameters described in Ref. 13. As in the past, the time increment and vortex magnitudes were adjusted so that plotting accuracy or better was retained throughout the calculations. The meanings of the various symbols used are given in the nomenclature.

Effect of Velocity Gradient on Vortex

The first flowfield to be analyzed consists of a single vortex embedded in a region whose velocity varies linearly with height, such that it approximates a velocity gradient caused by neighboring vortices or by a wind shear in the atmosphere. Such a flowfield has a constant value of vorticity throughout so that any convection of the background fluid does not alter the linear velocity gradient nor the ambient distribution of vorticity. If other velocity gradients were used, the background vorticity would not be a constant, and it would be necessary to monitor the convection of all of the vorticity in the calculations, thereby considerably complicating the analysis. For these reasons, the calculations were made only for a linear velocity gradient in the vertical direction of the lateral velocity such that

$$v(z) = \frac{z}{r_v} \frac{\Gamma_v}{2\pi r_v} V_{sh} \quad (3)$$

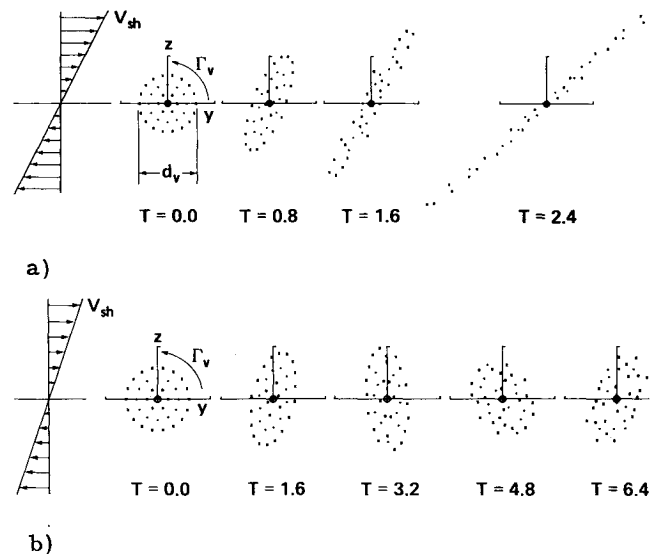


Fig. 3 Vortical region embedded in wind shear environment $\Gamma_v = 3.6 b U_\infty$. a) Sufficient wind shear to disperse core; $V_{sh} = +0.2$, $k = -1$; b) Insufficient wind shear; $V_{sh} = +0.20$, $k = -1$.

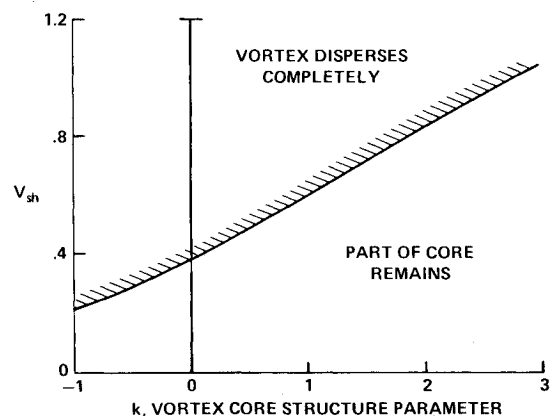


Fig. 4 Wind shear required to disperse vortex cores for a range of core structures.

where the dimensionless parameter V_{sh} is varied to simulate various amounts of shear. When $V_{sh}=1$, the velocity at the top of the vortical region ($y=0$, $z=r_v$) has a contribution from the shear field that is opposite to, and about equal to, that from the circulation in the vortex. The circulation contained inside the circle r_v , because of the background velocity field, then is related to that of the vortex by

$$\Gamma_{sh} = -V_{sh}\Gamma_v/2 \quad (4)$$

where $|\Gamma_v| = 3.6 b U_\infty$.

A series of numerical calculations then were made of the time-dependent motion of a vortical region in the shear environment. As in Ref. 13, the calculations were monitored for numerical error by evaluating periodically the first and second moments of vorticity and the Kirchhoff-Routh path function Wr . Since the point vortices are now embedded in a linear velocity field, the path function contains additional terms,¹⁴ so that it assumes the form

$$Wr = \sum_{i=1}^{N-1} \sum_{j=i+1}^N \left(\frac{\gamma_i \gamma_j}{4\pi} \right) \ln[(y_i - y_j)^2 + (z_i - z_j)^2] - \left(\frac{V_{sh}\Gamma_v}{4\pi r_v^2} \right) \sum_{i=1}^N z_i^2 \gamma_i \quad (5)$$

The influence of a shear environment on a vortical region is illustrated in Figs. 3a and 3b for a Rankine vortex ($k=-1$). In Fig. 3a, the shear was strong enough to disperse the core. In the second case (Fig. 3b), the value of the shear gradient was slightly less, so that, although the shape of the core fluctuates, it remains essentially intact and is not dispersed. The boundary (Fig. 4) between wind-shear values that do or do not disperse the core was determined by making successive numerical calculations to bracket the boundary for various values of the vortex core-structure parameter k . As expected, larger velocity gradients are required to disperse the more concentrated vortical regions. For example, when $k=3$ and $V_{sh} \approx 0.9$, the outer rings of point vortices were stripped off to leave the innermost ring essentially intact. In other cases, wherein $k \approx 2$ and $V_{sh} \approx 1$, the vortical regions first divides into two parts or forms an S-shaped curve that then disperses.

The results shown in Figs. 3 and 4 are typical of those in which the ambient shear opposes or slows the rotational velocity of the core. When the velocity gradient is reversed (V_{sh} negative), the initially round vortical regions are found to shrink in the z direction and to elongate slightly in the y direction, as shown in Fig. 5. However, values of V_{sh} as great as -2.0 did not disperse the vortex. It was concluded, therefore, that velocity gradients that enhance the rotation of a vortex will not disperse it, but ones that oppose the rotation will disperse it if the gradient is above the boundary indicated in Fig. 4.

Merging Conditions for Two Vortices

The vortex cores studied hereafter do not have a background vorticity, but depend entirely on the induced velocity field of other vortices for dispersion or merging. As in the previous section, numerical examples were calculated iteratively to determine the boundary between merging and nonmerging conditions. Now, however, the merging bound-

dary is a function of the core structure parameter k , the spacing of the vortices d_s , and the relative strengths of the cores Γ_1/Γ_2 , so that, rather than a single curve, a system of curves is needed to define the boundaries for the range of the several parameters to be studied. In order to limit the number of variables, the diameter d_v and the core structure parameter k were always made the same for the two cores.

Interaction of two vortex cores typical of those calculated to determine the merging boundaries are illustrated in Figs. 6 and 7. In the first case, two cores of equal size and strength are placed near one another, but are not touching. The circular distributions quickly distort, by a tuck and merge sequence, to form a single region with spiral-shaped remnants that slowly wrap around the outer part of the vortex. From Fig. 6, it can be seen that the centroids of vorticity for each core move toward each other and toward the origin, so that, at $T=6.4$, merger is near completion. At a slightly greater separation distance between the two vortex centers (Fig. 7), merger does not occur, even though the cores become elongated periodically as they orbit about one another. A series of such calculations were made to establish boundaries between merging and nonmerging conditions for the range of vortex spacings, strength ratios, and core structures shown in Fig. 8. In all of these calculations, the criterion used for merger was that the two cores become one, whether both or only one are distorted in the process.

The critical separation for merging when $k=-1$ and $\Gamma_1/\Gamma_2=1$ was found by Roberts and Chirstiansen⁶ to be

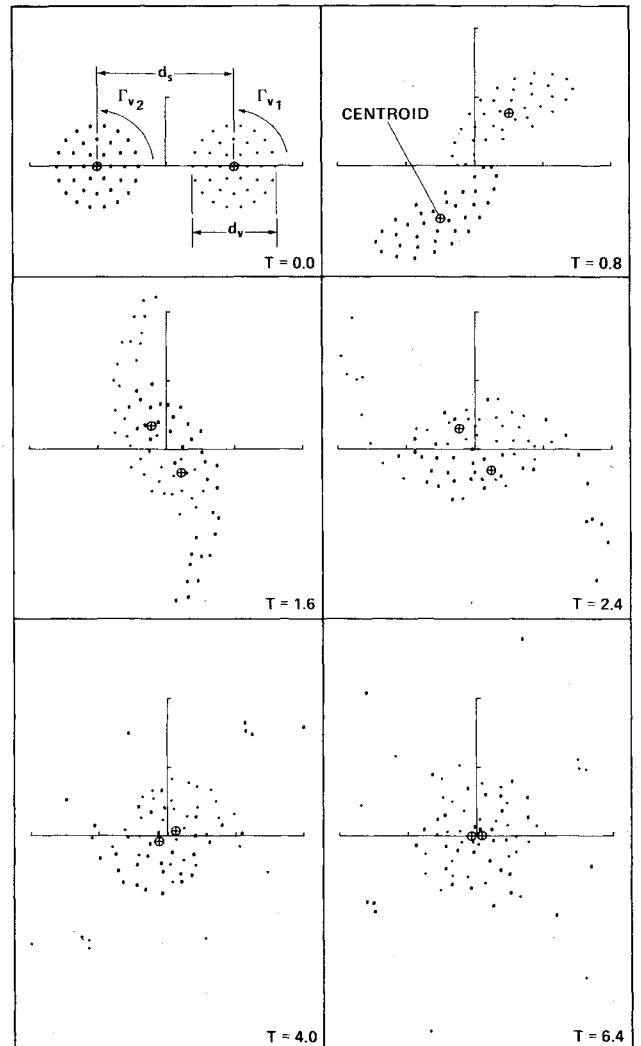


Fig. 6 Merging sequence predicted numerically for two Rankine vortices of equal strength; $\Gamma_2/\Gamma_1 = 3.6 b U_\infty$, $d_s = 1.7 d_v = 1.46 d_e$, $k = -1$.

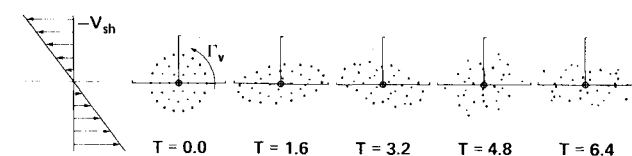


Fig. 5 Compression of vortex core by negative wind-shear environment; $V_{sh} = -0.5$, $k = -1$.

about 1.7, whereas the present numerical analysis (Fig. 8) indicates the value of d_s/d_v to be about 1.9. If however, the reference diameter for the vortex cores is defined not as the diameter of the outer ring of vortices but as $7/6$ times d_v , the present results agree with those of Ref. 6. The validity of this larger reference diameter for vortex interactions was pointed out to the author by J. D. Iversen of Iowa State University.† Upon reading the preprint version of this paper, he reasoned that, since the point vortices are distributed approximately uniformly on three concentric circles, they each represent a given cross-sectional area of the core. The reference or characteristic diameter for the core should then be based on the outer radius of the core area rather than on the radius of the outer circle of vortex centers. On the basis of such an argument, the proper or effective diameter d_e of the vortex cores studied here is $7/6$ times d_v . Both reference dimensions are presented in Figs. 6-17 for comparison purposes. A similar change in the shear parameter V_{sh} was not made, because its definition is arbitrary.

Merger of two vortical regions was noted to come about by several different processes. The tuck and wrap process shown in Fig. 6 was typical of many cases wherein the vortices had nearly the same strength and were closely spaced. These merging patterns resemble quite closely the theoretically predicted^{11,12} and the experimentally observed dye¹⁵ and smoke¹² flowfields presented in previous studies for the early stages of interactions. When one vortex was about ± 0.1 times as strong as the other, merger was accomplished by the weaker vortex being stretched and wrapped around the stronger one in the manner depicted in Fig. 10 of Ref. 3. Negative values of Γ_1/Γ_2 were observed to merge only by this process.

Another merging pattern that results when the theoretical parameters are set at $k = +2$ and $\Gamma_1/\Gamma_2 = 1$ was similar to a flow pattern observed in smoke flow visualization studies by Iversen† at Iowa State University. He found that vortices shed by two wings of elliptic planform interacted to form a new pattern of concentric rings, such as those shown in Fig. 9. It has been found in the present numerical studies, and in the various experiments mentioned, that a wide variety of merger patterns are possible. However, in the studies of two interacting cores, no combination was found to disperse the circulation in the way observed for the wind-shear examples of the previous section. For two vortices without wind shear,

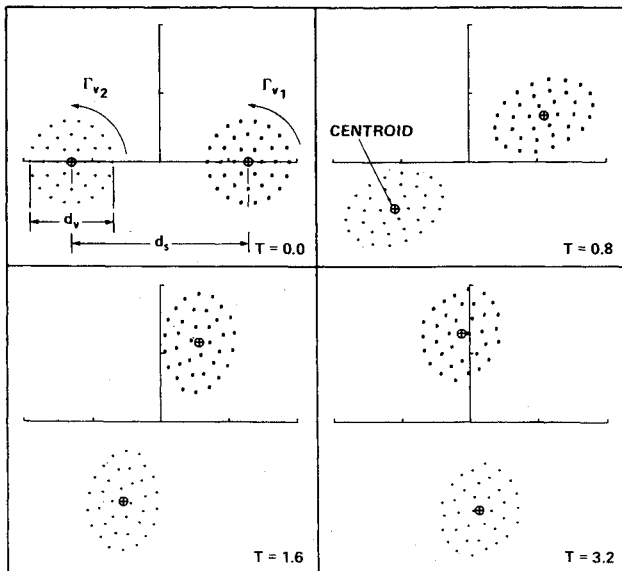


Fig. 7 Case where two Rankine vortices do not merge because spacing between them is too large, $\Gamma_1 = \Gamma_2 = 3.6b U_\infty$, $d_s = 2.2d_v = 1.89d_e$, $k = -1$.

†Private communication.

merger caused the content of one vortex to be wrapped around or rolled into the other (stronger) vortex so that the initial form of the concentric rings of point vortices was destroyed. The resulting vorticity distribution after merger is completed is approximately uniform near the center, and tapers off at the periphery of the region.

Interaction of Three Vortical Regions

The next step in a systematic study of the interaction of vortex cores is from two to three or more regions of vorticity to find out if configurations can be found that are particularly effective in dispersing vorticity. This study will be limited to two arrangements of three circular cores of the same size and on a common line of centers. In the first arrangement, the two outer vortices are positive and the center one negative, to find out how it responds to the velocity gradient in which it is em-

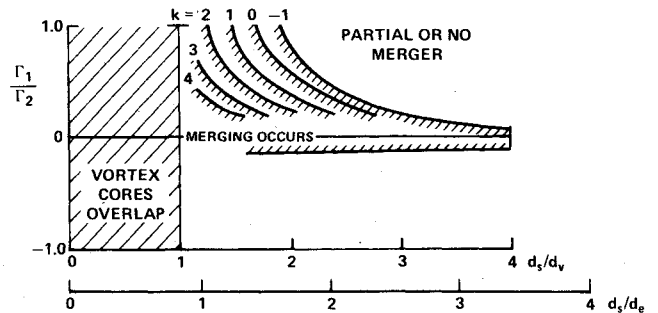


Fig. 8 Combinations of strength and spacing required for two vortex cores of the same diameter to merge.

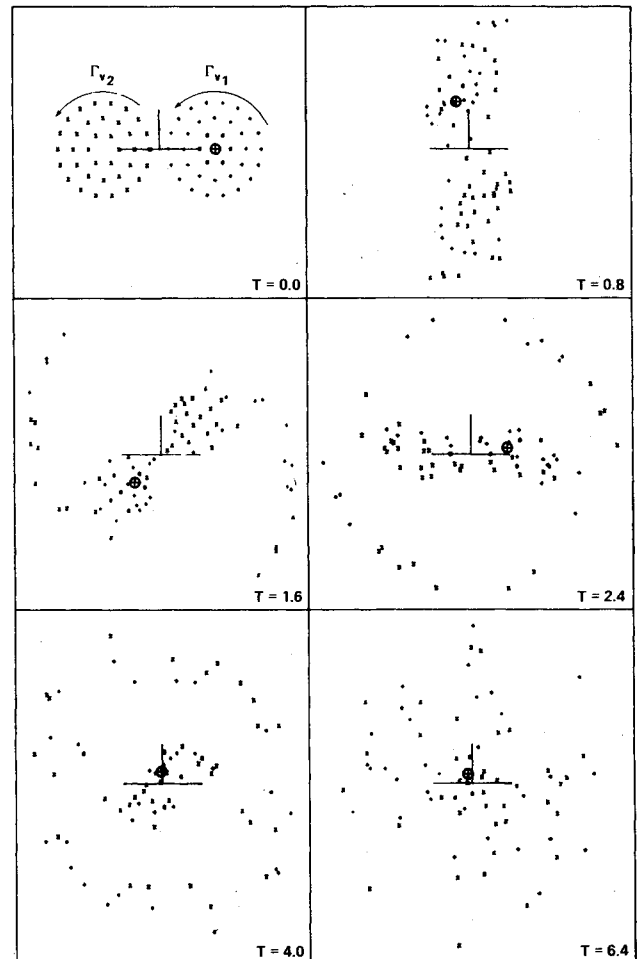


Fig. 9 Merging sequence leading to ring-type configuration of point vortices; $\Gamma_1 = \Gamma_2 = 3.6b U_\infty$, $k = +2$, $d_s = 1.17d_v = d_e$.

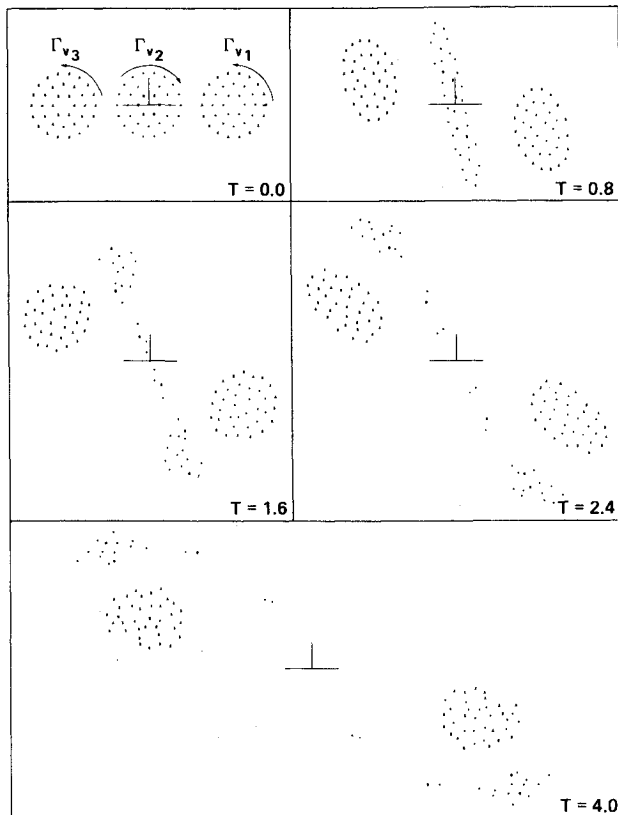


Fig. 10 Interaction of three vortical regions, $\Gamma_1 = -\Gamma_2 = \Gamma_3 = 3.6 b U_\infty$, $k = -1$, $d_s = 1.33 d_v = 1.14 d_e$.

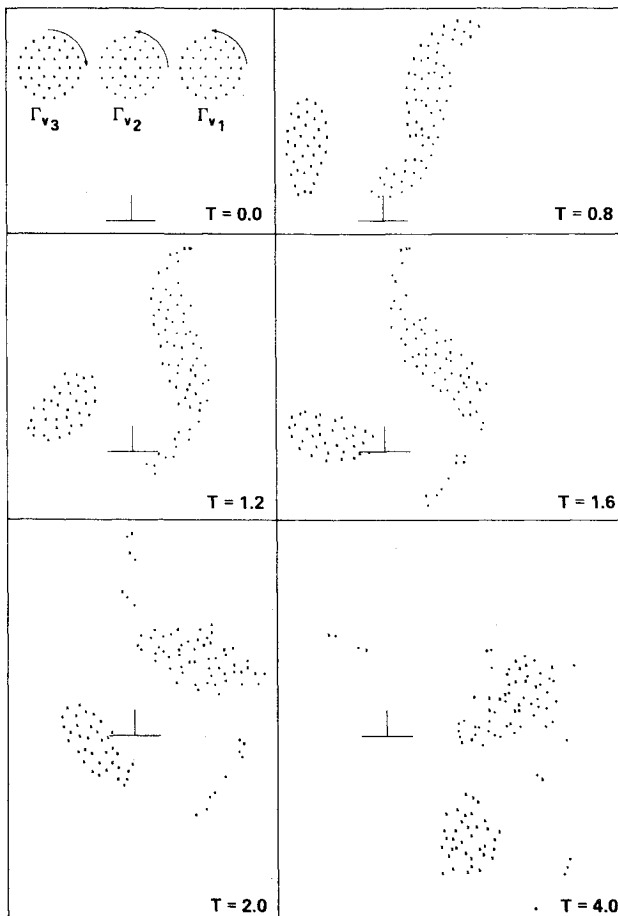


Fig. 11 Interaction of three vortical regions when the left vortex is opposite in sign to the other two; $\Gamma_1 = \Gamma_2 = -\Gamma_3 = 3.6 b U_\infty$, $k = -1$, $d_s = 1.33 d_v = 1.14 d_e$.

bedded. As shown in Fig. 10, the middle core is divided in half by being stretched out, in somewhat the same manner as that observed in Fig. 3a, and then wrapped around the two outer ones. These two newly formed regions then move off in a circular orbit typical of an unequal vortex pair. Such a division (or dispersion of vorticity) occurs for vortices of equal magnitude if the two outer vortices are spaced less than 6 diam apart (or 3 diam from the center one). This is surprising, since any two of the vortex cores do not distort or disperse one another at all (at these distances), unless the third vortex is present. If the center vortex is made weaker, it is more likely to be divided, but, if it is made stronger than the outer vortices, the center vortex stays intact and the structure of the two outer cores is modified.

An interaction typical of the second arrangement wherein the negative vortex is now on the left is shown in Fig. 11. The one odd vortex is not divided in this case, but the two vortices of the same sign quickly merge to form a new stronger vortex. A kind of dispersion then occurs, because the two remaining regions convect their net circulation across the flowfield on a circular orbit. It is expected that viscosity, turbulence, and three-dimensional interactions such as linking then would cause the cores to combine to form a single core with a net strength equal to one of the original positive cores. Once again, changes in the space between centers or in the relative strengths of the cores affects their motion and any merger or dispersion that might occur.

Applications to Lift-Generated Wakes

Wake Alleviation Techniques

The foregoing subsections discussed the interaction of vortical regions to gain an understanding of merger and dispersion by inviscid convection. Before extending these results to multiple vortex pairs in order to better simulate lift-generated wakes, some desired features in a wake which make it less hazardous are discussed. Merger of two vortical regions in itself is an insufficient criterion, because the resulting vortex contains more circulation and may cause larger rolling moments on an encountering wing. Hence, as mentioned in the introduction, the interactions sought are those that combine, spread, or disperse the circulation, so that the net rolling moment imposed on an encountering aircraft is reduced by at least a factor of two (hopefully 5 or 10) below that of wakes shed by large conventional aircraft. A discussion of some inviscid mechanisms for accomplishing this are given in Ref. 16. Of interest here are two-dimensional interactions that: 1) spread or disperse the circulation over a large region (shown to be possible with wind shear), and 2) combine vortices of opposite sign to reduce the magnitude of concentrations of circulation in wake. For example, the "sawtooth loading" appears to be one way to combine vortices of opposite sign so that motions occur that disperse the wake. Also, a discussion of a centroid of circulation concept given in Ref. 16 indicates how combinations of cores of opposite sign, by two-dimensional merger or three-dimensional linking, can bring about reductions in wake hazard. The sections to follow therefore present some results for multiple vortex pairs to simulate complete aircraft wakes. These cases were restricted to Rankine-type cores ($k = -1$) of the same diameter to limit the large number of possible variations. Several promising vortex configurations were found, but an optimum or highly effective arrangement has not yet been identified.

Vortex Pair in Wind Shear

The effect of velocity gradient or wind shear on a vortex pair (Fig. 12) is about the same as it was when the positive and negative cores were analyzed separately or in isolation. As in Figs. 3 and 5, the positive velocity gradient disperses the positive vortex but appears to concentrate the negative vortex. It seems then that, if an aircraft were to pass through a region

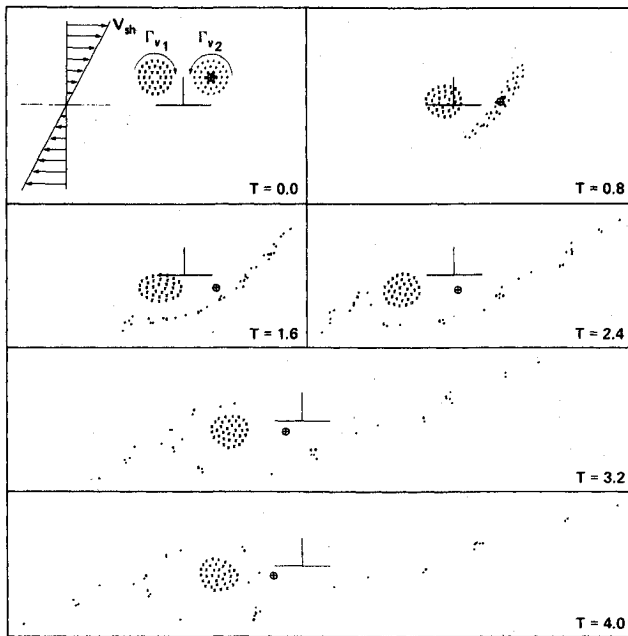


Fig. 12 Effect of wind shear on a vortex pair; $\Gamma_1 = -\Gamma_2$, $V_{sh} = +0.26$, $k = -1$, $d_s = 1.7 d_v = 1.46 d_e$.

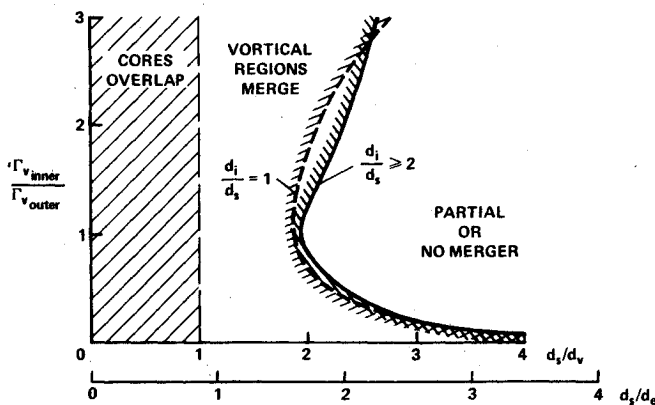


Fig. 13 Merging guidelines for vortex pairs of the same sign and diameter as a function of spacing and strength ratio.

with wind shear perpendicular to its path, the two-vortex wake could be changed from a vortex pair to a single core, which appears to be more hazardous because of its compression in the vertical direction caused by the wind shear. Visual observations have been made of such occurrences,¹⁷ but measurements to confirm the dispersion of one of the vortices have not been made.

Interaction of Two Vortex Pairs

Vortex pairs of same sign. The presence of a centerplane or plane of symmetry causes differences in the merger process when the spacing d_i between the two innermost vortices is less than about twice the spacing d_s of the outer vortices (Fig. 13). Unfortunately, closer spacing (such as $d_i/d_s = 1.0$) tends to make the vortices less likely to merge, requiring a slightly different guideline curve for each spacing ratio d_i/d_s less than two. Since no new merger processes were found, only the guideline curves shown in Figs. 13 are presented to indicate how the large span results ($d_i/d_s \geq 2$) were modified by finite spacing. Since the calculation now depends on whether the stronger vortex is inboard or outboard, the ordinate must now include ratios of vortex strength, ($\Gamma_{inner}/\Gamma_{outer} = \Gamma_i/\Gamma_o$) greater than one. The crossing of the two curves in Fig. 13 at about $\Gamma_i/\Gamma_o = 2.8$ is caused by a change in the merger process,

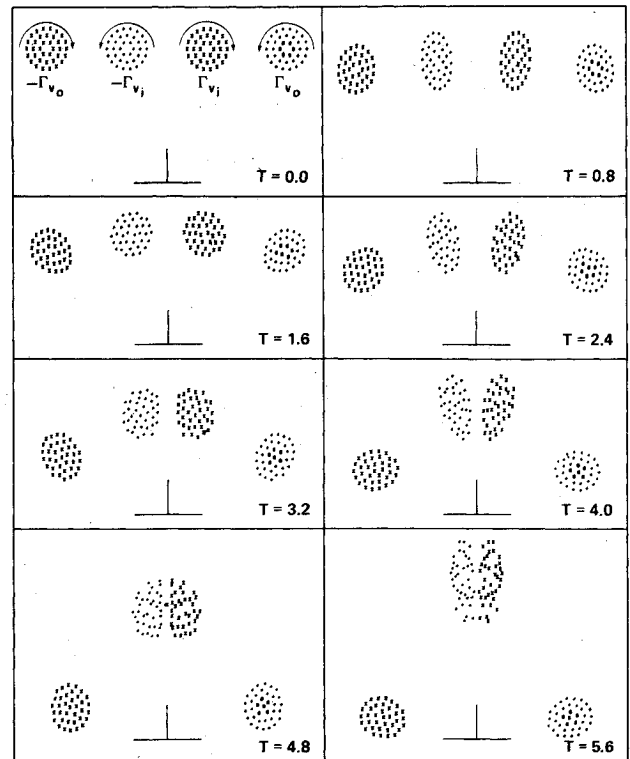


Fig. 14 Interaction of two vortex pairs of opposite sign and of the same strength; $\Gamma_i = -\Gamma_o = -3.6 b U_\infty$, $d_i = d_s$, $d_s = 2.0 d_v = 1.71 d_e$, $k = -1$.

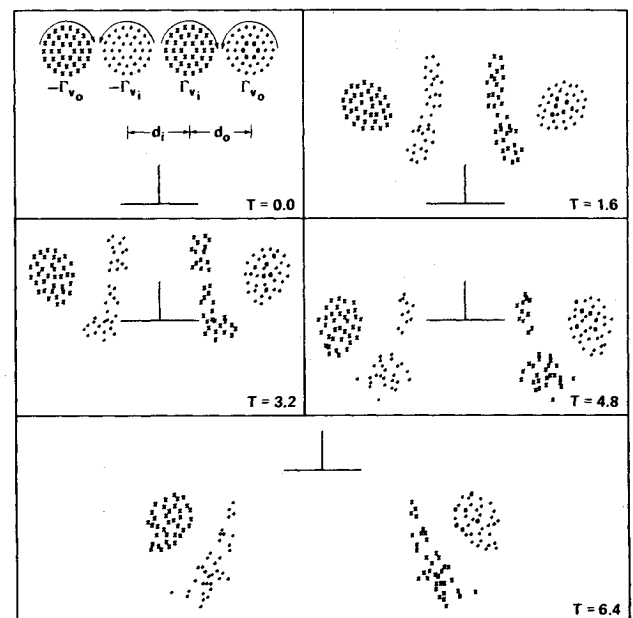


Fig. 15 Interaction of two vortex pairs of opposite strength designed to translate downward at the same velocity; $\Gamma_o = +3.6 b U_\infty$, $\Gamma_i = -2.8 b U_\infty$, $d_s = 1.33 d_v = 1.14 d_e$, $k = -1$.

wherein the centerplane helps to disperse the vortices around the stronger inner vortex.

Two vortex pairs of opposite sign. If two vortices of the same sign merge, the newly formed vortical region is larger and contains more vorticity, so that it is not obvious whether the velocities and the associated hazard are reduced or increased. However, when vortices of opposite sign combine, the net circulation is reduced so that a lower hazard would be expected. Interactions of this kind are needed to achieve the alleviation possible when the centroid of vorticity y is out-

board of the wing tip.¹⁶ In the absence of a centerplane (Fig. 8), it was found that two vortices, opposite in sign, combine only when one is at least five times as strong as the other. Two cases are now presented that illustrate how the nonmerging situation is modified when the span between the vortices is reduced below $d_i/d_s = 2$. In Fig. 14, the strengths of the vortex pairs are of the same magnitude but opposite in sign. From an initially uniform spacing, the vortices move inward and downward until the inboard vortices come together at the centerplane to form a nearly circular region. Turbulence, viscosity, and three-dimensional effects probably would cause this newly formed vorticity group to dissipate. Such interactions have been observed by Ciffone, who used dye flow visualization techniques to investigate the wakes of models of the Boeing 747¹⁵ and DC-10.⁸ These experimental results and the limited number of numerical examples calculated so far, indicate that such vortex motions occur for a wide range of parameters. Unfortunately, the outboard or wing tip vortices are not modified by the vortex dissipation at the centerplane, and therefore remain untouched for alleviation. The calculations indicated that if the center spacing is too large, the vortices on each side move independently. If the center space is too small (or the strengths too great), the inboard vortices quickly move away from the outboard ones. The vortex motion guidelines provided by point vortex paths (e.g., Fig. 2.2 of Donaldson and Bilanin¹¹) can be used to estimate the limits over which the vortex strengths and spacing will yield inward moving vortices.

In the second example (Fig. 15), Γ_i/Γ_o was chosen so that the downward velocity of the centers of the four vortices was the same in order to approximate the "stepped span loading".¹³ Once set in motion, the inboard vortices form a crescent shape about the outboard vortices. The two new groups of vorticity then move downward and outboard as a unit, which should lead to neutralization of the circulation (i.e., $\Sigma\gamma \approx 0$). Similar results can be achieved with other spacing ratios, but, if the vortices are much closer to the centerplane, part of the crescent formed by the inboard vortices stays behind as a new and separate pair. The combined strength of the outboard moving vortices is not, then, neutralized to the extent possible with the configuration in Fig. 15. If the vortices are separated by too great an amount for their diameter, the inboard ones do not take on a crescent shape and all of the vortices move without modification, as if they were point vortices. The vortex interaction shown in Fig. 15 indicates that it may be possible to develop at least partial alleviation with two vortex pairs because the net circulation, after mixing in the outboard vortex group, drops to about 22% of the original strength of the outboard vortex by itself.

Interaction of Three Vortex Pairs

The dispersion and vortex pairing indicated by the results in Figs. 10 and 11 for three vortical regions suggest that usable alleviation may be achieved with three vortex pairs if the addition of a centerplane is not adverse. Only the cases wherein one vortex pair is negative will be presented, and, as before, only Rankine-type ($k = -1$) cores of the same diameter are analyzed. Consider first the case of the middle vortex pair that is opposite to the other two (Fig. 16). The initial redistribution of point vortices is noted to be quite similar to the three-vortex case shown in Fig. 10. As time progresses, however, the inner groupings now impact each other at the centerplane, so that the circulation tends to be neutralized. The two outboard moving vortical regions then have a net strength of about 5/9 of the original strength of a core, because of the reduction in net circulation caused by the opposite vortices.

In the second situation (Fig. 17), the wake is composed of three pairs wherein the most inboard pair is opposite in strength to the two outboard pairs. Although the presence of a centerplane does not change the gross character of the flow-

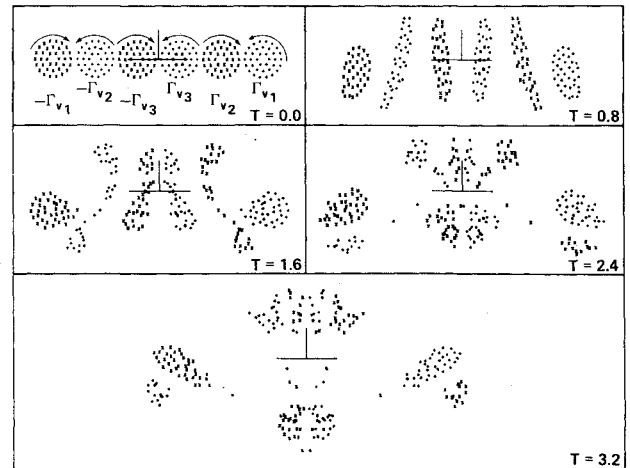


Fig. 16 Interaction of three vortex pairs when center pair is negative; $\Gamma_1 = -\Gamma_2 = \Gamma_3 = 3.6 b U_\infty$, $d_s = 1.17 d_v = d_e$, $k = -1$.

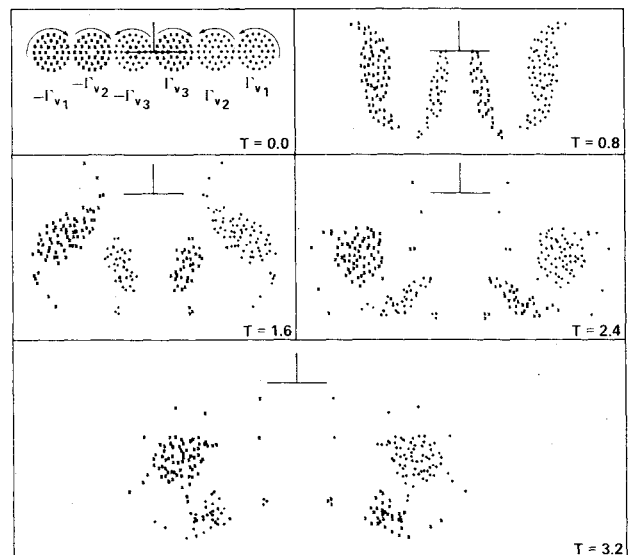


Fig. 17 Interaction of three vortex pairs when inboard pair is negative; $\Gamma_1 = \Gamma_2 = -\Gamma_3 = 3.6 b U_\infty$, $d_s = 1.17 d_v = d_e$, $k = -1$.

field, some of the orderliness of the point vortex arrangement in Fig. 11 is lost in Fig. 17. The merger of the two outer cores without dispersing causes the net circulation, after $T = 3.2$ on each side of the centerplane, to be about twice as large as that for the wake considered in Fig. 16.

Other wakes with 3 and 4 vortex pairs also were calculated, including those designed to move downward at the same velocity as prescribed by stepped loading.¹³ None of these other cases had vortex interactions that were significantly different from those already presented. Other configurations not considered may be more effective, since a number of combinations of parameters remain to be considered.

Concluding Remarks

Various ways in which vortical regions interact have been explored by numerical analysis of the inviscid time-dependent convective motions of the vorticity. The objective was to find those configurations that disperse or neutralize lift-generated circulation so that the hazard posed by wakes of aircraft might be reduced. It was found that a vortex core can be made to disperse when it is placed in a velocity shear region of sufficient strength. If the shear field is provided by vortices, their signs should alternate along the span (e.g., sawtooth loading) so that each vortex finds itself in a velocity gradient. Proper

⁸Ciffone, unpublished data.

adjustment of the vortex strengths and spacings can then be carried out so that the cores split into smaller segments and disperse, or form groups with nearly zero net circulation which tend to neutralize the wake.

As expected, Rankine cores (i.e., cores with uniform distribution of vorticity) are more likely to merge or disperse than cores with their circulation concentrated near the vortex center. The calculations made by Donaldson and Bilanin show that turbulence and viscosity diffuse concentrated cores, so that vortices in an experiment grow to a size whereby they are more apt to merge or disperse than indicated by the present analysis. Therefore, the merging guidelines estimated here are probably conservative, and will become more so as the wake ages.

References

- ¹Dunham, E. R., Jr., "Model Tests of Various Vortex Dissipation Techniques in a Water Towing Tank," NASA Langley Working Paper LWP-1146, Jan. 1974.
- ²Corsiglia, V. R. and Dunham, R. E., "Aircraft Wake-Vortex Minimization by use of Flaps," *NASA Symposium on Wake Vortex Minimization*, NASA SP-409, 1976, pp. 303-336.
- ³Corsiglia, V. R., Rossow, V. J., and Ciffone, D. L., "Experimental Study of the Effect of Span Loading on Aircraft Wakes," *Journal of Aircraft*, Vol. 13, Dec. 1976, pp. 968-973.
- ⁴Tymczyszyn, J. J., and Barber, M. R., "Recent Wake Turbulence Flight Test Programs," SETP 1974 Report to the Aerospace Profession—Eighteenth Symposium Proceedings. Society of Experimental Test Pilots, Sept. 1974, pp. 52-68.
- ⁵Moore, D. W. and Saffman, P. G., "Structure of a Line Vortex in an Imposed Strain," *Aircraft Wake Turbulence and Its Detection*, edited by J. H. Olsen et al., Plenum Press, New York, 1971, pp. 339-354.
- ⁶Roberts, K. V. and Christiansen, J. P., "Topics in Computational Fluid Mechanics," *Computer Physics Communications, Supplement*, Vol. 3, Sept. 1972, pp. 14-32.
- ⁷Christiansen, J. P., "Numerical Simulation of Hydrodynamics by the Method of Point Vortices," *Journal of Computational Physics*, Vol. 13, Nov. 1973, pp. 363-379.
- ⁸Christiansen, J. P. and Zabusky, N. J., "Instability, Coalescence and Fission of Finite-Area Vortex Structures," *Journal of Fluid Mechanics*, Vol. 61, Pt. 2, Nov. 6, 1973, pp. 219-243.
- ⁹Winant, C. D. and Browand, F. K., "Vortex Pairing: the Mechanism of Turbulent Mixing-Layer Growth at Moderate Reynolds Number," *Journal of Fluid Mechanics*, Vol. 63, Pt. 2, April 1974, pp. 237-255.
- ¹⁰Moore, D. W. and Saffman, P. G., "The Density of Organized Vortices in a Turbulent Mixing Layer," *Journal of Fluid Mechanics*, Vol. 69, Pt. 3, June 1975, pp. 465-473.
- ¹¹Donaldson, C. du P. and Bilanin, A. J., "Vortex Wakes of Conventional Aircraft," AGARDograph No. 204, May 1975.
- ¹²Bilanin, A. J., Teske, M. E., Donaldson, C. du P., and Snedeker, R. S., "Viscous Effects in Aircraft Trailing Vortices," *NASA Symposium on Wake Vortex Minimization*, NASA SP-409, 1976, pp. 55-122.
- ¹³Rossow, V. J., "Theoretical Study of Lift-Generated Vortex Wakes Designed to Avoid Roll Up," *AIAA Journal*, Vol. 13, April 1975, pp. 476-484.
- ¹⁴Lin, C. C., "On the Motion of Vortices in Two Dimensions," No. 5, *Applied Mathematics Series*, The University of Toronto Press, Toronto, 1943.
- ¹⁵Ciffone, D. L., "Vortex Interactions in Multiple Vortex Wakes Behind Aircraft," *Journal of Aircraft*, to be published.
- ¹⁶Rossow, V. J., "Inviscid Modeling of Aircraft Trailing Vortices," *NASA Symposium on Wake Vortex Minimization*, NASA SP-409, 1976, pp. 4-54.
- ¹⁷Tombach, I., "Observations of Atmospheric Effects of Vortex Wake Behavior," *AIAA Journal of Aircraft*, Vol. 10, Nov. 1973, pp. 641-647.

From the AIAA Progress in Astronautics and Aeronautics Series . . .

INSTRUMENTATION FOR AIRBREATHING PROPULSION—v. 34

Edited by Allen Fuhs, Naval Postgraduate School, and Marshall Kingery, Arnold Engineering Development Center

This volume presents thirty-nine studies in advanced instrumentation for turbojet engines, covering measurement and monitoring of internal inlet flow, compressor internal aerodynamics, turbojet, ramjet, and composite combustors, turbines, propulsion controls, and engine condition monitoring. Includes applications of techniques of holography, laser velocimetry, Raman scattering, fluorescence, and ultrasonics, in addition to refinements of existing techniques.

Both inflight and research instrumentation requirements are considered in evaluating what to measure and how to measure it. Critical new parameters for engine controls must be measured with improved instrumentation. Inlet flow monitoring covers transducers, test requirements, dynamic distortion, and advanced instrumentation applications. Compressor studies examine both basic phenomena and dynamic flow, with special monitoring parameters.

Combustor applications review the state-of-the-art, proposing flowfield diagnosis and holography to monitor jets, nozzles, droplets, sprays, and particle combustion. Turbine monitoring, propulsion control sensing and pyrometry, and total engine condition monitoring, with cost factors, conclude the coverage.

547 pp. 6 x 9, illus. \$14.00 Mem. \$20.00 List

TO ORDER WRITE: Publications Dept., AIAA, 1290 Avenue of the Americas, New York, N. Y. 10019